AD-A033 795 NAVAL ELECTRONICS LAB CENTER SAN DIEGO CALIF F/G 17/5
PROPERTIES OF PHOTODETECTORS (PHOTODETECTOR SERIES, 97TH REPORT--ETC(U)
SEP 76 D C ARRINGTON, R L BATES, W L EISENMAN

UNCLASSIFIED NELC/TR-2014 NL

| OF |
AD
A033795

END
DATE
FILMED
2-77

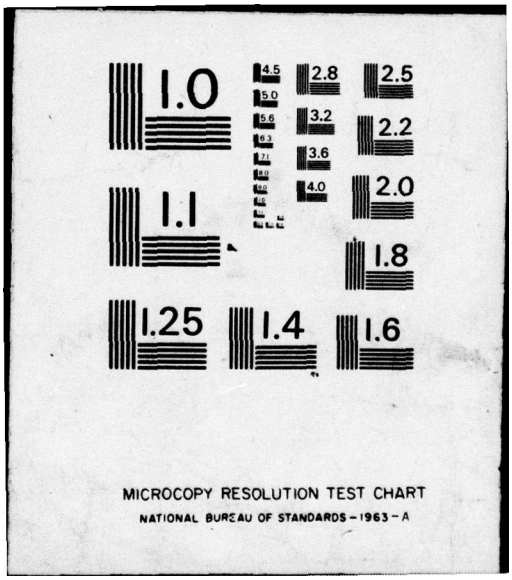
1.0
1.1
1.25
1.4
1.6
1.8
2.0
2.2
2.5
2.8
3.2
3.6
4.0
4.5
5.0
5.6
6.3
MICROCOPY RESOLUTION TEST CHART
NATIONAL BUREAU OF STANDARDS - 1963 - A

[redacted]

12

PROPERTIES OF PHOTODETECTORS

(Photodetector Series, 97th Report)

Spatial Sensitivity of LWIR Detectors

September 1976

Electronic Material Sciences Division
Research and Development, January–June 1976

Prepared for
ARMY MATERIALS AND MECHANICS RESEARCH CENTER

[redacted]

NAVAL ELECTRONICS LABORATORY CENTER
SAN DIEGO, CALIFORNIA 92152

UNCLASSIFIED

SECURITY CLASSIFICATION OF THIS PAGE (When Data Entered)

REPORT DOCUMENTATION PAGE

READ INSTRUCTIONS BEFORE COMPLETING FORM

1. REPORT NUMBER: NELC Technical Report 2014 (TR 2014)
2. GOVT ACCESSION NO. (14)
3. RECIPIENT'S CATALOG NUMBER: NELC/TR-2014

4. TITLE (and Subtitle): (6) PROPERTIES OF PHOTODETECTORS (Photodetector Series, 97th Report). Spatial Sensitivity of LWIR Detectors.
5. TYPE OF REPORT & PERIOD COVERED: (9) Research and Development rept. January – June 1976.
6. PERFORMING ORG. REPORT NUMBER

7. AUTHOR(s): (10) D.C./Arrington, R.L./Bates, W.L./Eisenman, M.H./Sweet
Electronic Material Sciences Division
8. CONTRACT OR GRANT NUMBER(s)

9. PERFORMING ORGANIZATION NAME AND ADDRESS
Naval Electronics Laboratory Center
San Diego, CA 92152
10. PROGRAM ELEMENT, PROJECT, TASK AREA & WORK UNIT NUMBERS
63304A 0, ARMY
(NELC T301)

11. CONTROLLING OFFICE NAME AND ADDRESS
Army Materials and Mechanics Research Center
12. REPORT DATE: (11) September 1976
13. NUMBER OF PAGES: 24 (12) 22p.

14. MONITORING AGENCY NAME & ADDRESS (if different from Controlling Office)
15. SECURITY CLASS. (of this report): UNCLASSIFIED
15a. DECLASSIFICATION/DOWNGRADING SCHEDULE

16. DISTRIBUTION STATEMENT (of this Report)

Approved for public release; distribution is unlimited.

17. DISTRIBUTION STATEMENT (of the abstract entered in Block 20, if different from Report)

18. SUPPLEMENTARY NOTES

19. KEY WORDS (Continue on reverse side if necessary and identify by block number)

Infrared detectors – Properties
Infrared photodetectors – Properties
Photodetectors
Semiconductors (materials) – Properties

20. ABSTRACT (Continue on reverse side if necessary and identify by block number)

The results of measurements of the spatial sensitivities of several low-background photoconductive HgCdTe detector elements are presented. Data show in all cases substantial variations in signal amplitude over the sensitive area of the detector. Measurements on several extrinsic low-background detectors show that the spatial characteristics are dependent upon the geometry of the bias field. Few extrinsic detectors utilizing transparent electrodes have been measured but the data collected indicate that this type of detector can have good performance characteristics and uniform spatial sensitivity.

DD FORM 1 JAN 73 1473 EDITION OF 1 NOV 65 IS OBSOLETE
S/N 0102-LF-014-6601

UNCLASSIFIED 403 940
SECURITY CLASSIFICATION OF THIS PAGE (When Data Entered)

FOREWORD

This report, prepared as part of the Joint Services Infrared Sensitive Element Testing Program, is the 97th in a series concerned with the various physical properties of photodetectors. This series of reports is intended to keep the users of infrared detectors abreast of state-of-the-art devices.

OBJECTIVE

Develop techniques and apparatus for measuring the performance characteristics of new or improved infrared photodetectors. Define and measure the pertinent detector parameters such as spectral response, noise spectra, frequency response, and noise equivalent power. Report the resultant data in suitable format to the Department of Defense, other governmental agencies, and their contractors.

RESULTS

Spatial sensitivity measurements have been made on a number of intrinsic and extrinsic photoconductive detectors. The measurements were made using a newly developed apparatus capable of generating the appropriate background photon flux level and wavelength.

ADMINISTRATIVE INFORMATION

Work was done from January to June 1976 by the Infrared Devices Branch of the Electronic Material Sciences Division under program element 63304A, project 0, task ARMY (NELC T301), for the Army Materials and Mechanics Research Center. This report is coauthored by DC Arrington, RL Bates, WL Eisenman, and MH Sweet and was approved for publication September 1976.

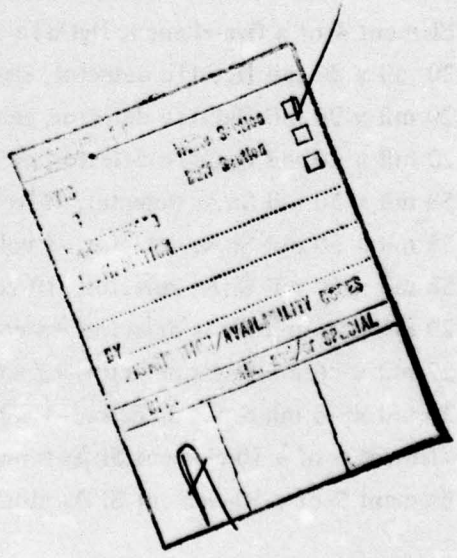

CONTENTS

ILLUSTRATIONS

TABLE

INTRODUCTION

The use of infrared detectors in space sensors has created a need to characterize the uniformity of response over the sensitive area of the detector under low-background photon flux environments. A low-background, spot-scanning apparatus has been built and several types of extrinsic and intrinsic detectors have been measured. The spot-scanning apparatus will be discussed briefly and data describing the sensitivity contours of several low-background detectors will be presented.

SPOT-SCANNER APPARATUS

The spot scanner consists of four basic parts. A cryogenic Dewar provides the necessary environment to cool the detector being measured and to cool radiation shields that constitute a cold optical cavity. The cold optical cavity surrounds the detector and optical system and maintains the low infrared (IR) background photon flux necessary for the measurement. The optical system, consisting of a PbSnTe light-emitting diode (LED), integrating cavity, pin-hole aperture, and Ge lenses, produces a small spot of IR radiation on the surface of the detector. An x-y drive mechanism translates the entire optical system to scan the spot over the plane of the detector.

The performance characteristics of the spot scanner are summarized in table 1.

TABLE 1. SPOT-SCANNER CHARACTERISTICS.

Background photon flux	$<10^8$ (photon/s-cm^2)
Optical wavelength	~10 (μm)
Spot size	60 (μm dia)
Scan length	10 (mm, x and y)
Focus adjustment	3 (mm)
Mechanical repeatability	~10 (μm, y-axis)
Detector operating temperature	4 to 20 (K)
Cool down time	6½ (h, 300 to 4 K)
Hold time	2 (h)

The scan length for both x- and y-axes is 10 millimetres. The cold optical system produces a spot about 60 micrometres in diameter at a wavelength of approximately 10 micrometres. Mechanical repeatability is on the order of 10 micrometres. The z-axis provides a focus adjustment of 3 millimetres. Measurements made with a calibrated detector show that the background is less than 10^8 photons/s-cm^2. The diode radiation source can be modulated at any frequency between 2 and 1000 Hz. Cool-down time is about 6½ hours and Dewar hold time is 2 hours. The apparatus can be refilled with helium in about 5 minutes without interrupting measurements.

Figure 1 is an external view of the spot-scanner assembly. At the bottom are the x-y indexing motors, drive screws, and precision linear-motion stages. The lower half of the Dewar contains the scanning mechanism and optical system. The section above the vacuum flange is a standard liquid helium-cooled Dewar.

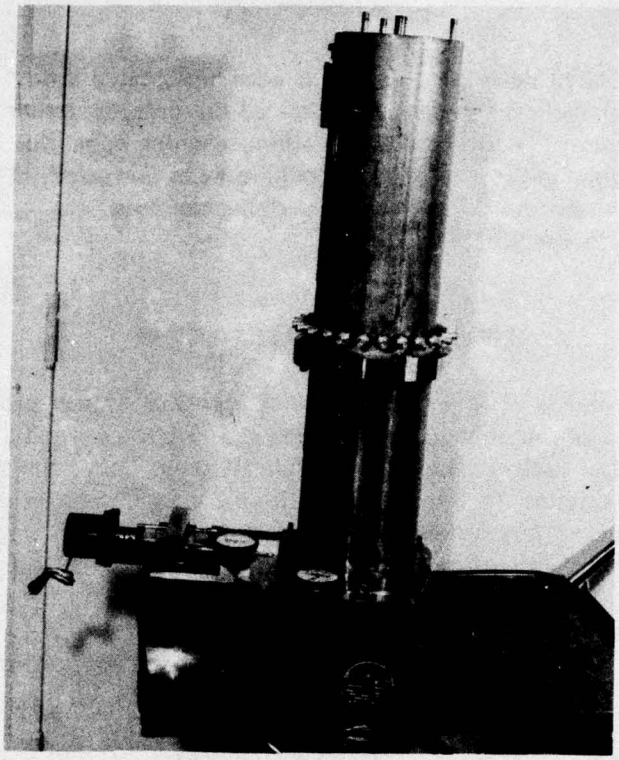

Figure 1. External view of the spot-scanner apparatus.

The data are obtained one line at a time by scanning the spot along the y-axis. The entire sensitive area of the detector is measured by generating line scans at many positions along the x-axis. The apparatus is capable of generating a number of scan patterns but the "scan in y, step in x" pattern is normally used. Each scan along the y-axis is made in the same direction to minimize backlash. For all the data in this report, the velocity of the spot in the y-direction was made small enough to allow the detector signal to reach equilibrium.

The IR radiation is modulated in the form of a symmetrical square wave. The electrical signal from the detector is amplified and then passed through a narrow-band filter tuned to the modulation frequency. A modulation frequency of 10 Hz was used for the data presented here. Most of the measurements were made with a signal-to-noise ratio of 10^2 to 10^3 in a 1-Hz bandwidth. After passing through the narrow-band filter, the detector signal is rectified, filtered, and sent to an automatic data processing (ADP) system. The rectified signal is digitized and stored in the form of signal amplitude as a function of spot position in the x-y plane. The ADP system also controls the x- and y-drive motors on the spot scanner and can automatically scan a detector or array of detectors.

The ADP system can output the accumulated data in two formats. A pseudo three-dimensional format showing signal amplitude distribution over the x-y plane can be generated using an x-y plotter. This format can be generated automatically and provides a simple qualitative description of the detector. A "sensitivity contour" format

can be produced to obtain a more quantitative description of the detector. Unfortunately, due to system hardware limitations, this format must be plotted by hand. Figure 2 shows data plotted in the two formats.

DATA

Measurements of spatial sensitivity have been made on a large number of detectors. These detectors are representative of several types and several manufacturers. For this report, the detectors have been divided into three groups:

(1) photoconductive HgCdTe

(2) extrinsic silicon with lateral electrodes (electric field perpendicular to direction of incident radiation)

(3) extrinsic silicon with transparent electrodes (electric field parallel to incident radiation).

Data are presented for several detectors of each type.

PHOTOCONDUCTIVE HgCdTe

The data shown in figures 3 and 4 are for two detectors (#1 and 2) of a 6-element array. This array (U-1) was manufactured from a single slab of HgCdTe. The nominal dimensions of the geometrical area are 0.012″ X 0.023″. In both cases the spatial sensitivity is not uniform and in the case of detector #2, one half of the detector is relatively insensitive.

The data shown in figures 5, 6, and 7 are for three individual detectors out of a total of four which were on a common mount. Detector S-14-32-H2 #2 had geometrical dimensions of 0.020″ X 0.020″, and detectors S-12-49 #2 and S-12-49 #3 had dimensions of 0.040″ X 0.040″. Again, the spatial sensitivity is nonuniform and, in the cases of the two 0.040″ X 0.040″ detectors, a large fraction of the geometrical area is quite insensitive.

Detectors S-14-39 #4 and S-14-39 #5, whose spatial sensitivities are shown in figures 8 and 9, were two individual detectors from a total of five on a common mount. Figures 10 and 11 show data on two other individual detectors from a group of five. Figures 12, 13, and 14 show data on three of six individual detectors. All detectors presented in figures 8 through 14 had geometrical dimensions of 0.020″ X 0.020″.

EXTRINSIC SILICON–LATERAL ELECTRODES

Data are shown for two detectors, ELMS 200 and HST 036, both of which are arsenic-doped silicon detectors. Detector dimensions are 0.058″ X 0.050″ X 0.080″ for ELMS 200 and 0.029″ X 0.076″ X 0.040″ for HST 036. The first two dimensions represent the active surface and the third dimension is the thickness of the devices. Both detectors are soldered to a metallic mount which is used as the ground bias electrode. The second electrode is soldered to the opposite side. This mounting procedure renders two surfaces insensitive to infrared radiation but leaves the other four surfaces exposed and sensitive. These exposed surfaces, together with reflecting metallic surfaces below

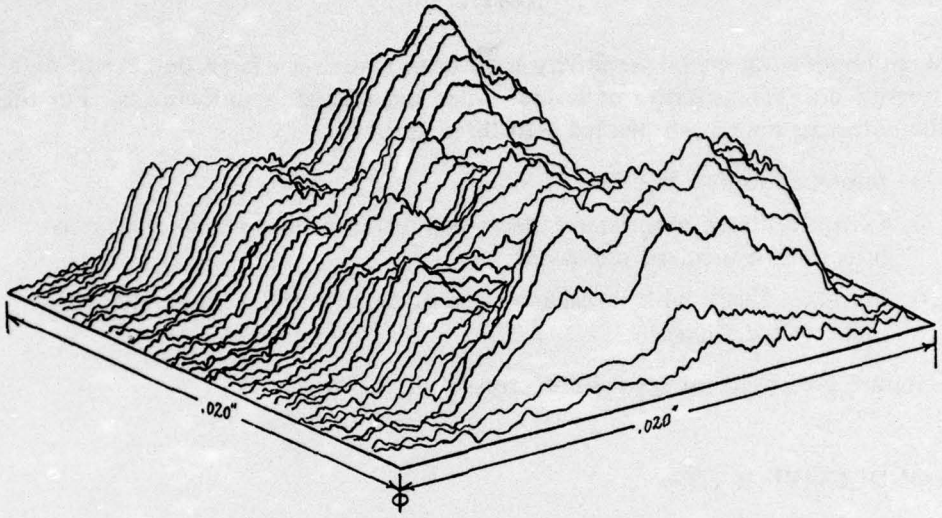

Figure 2-A. Pseudo three-dimensional data format.

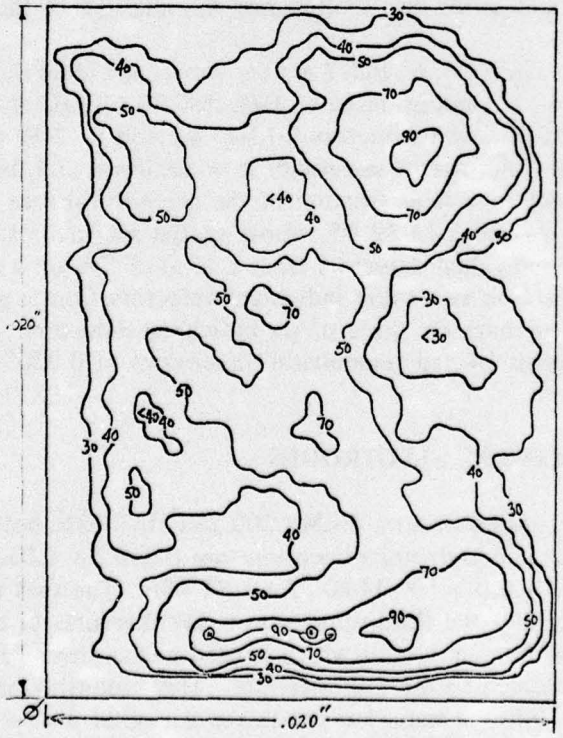

Figure 2-B. Sensitivity contour data format.

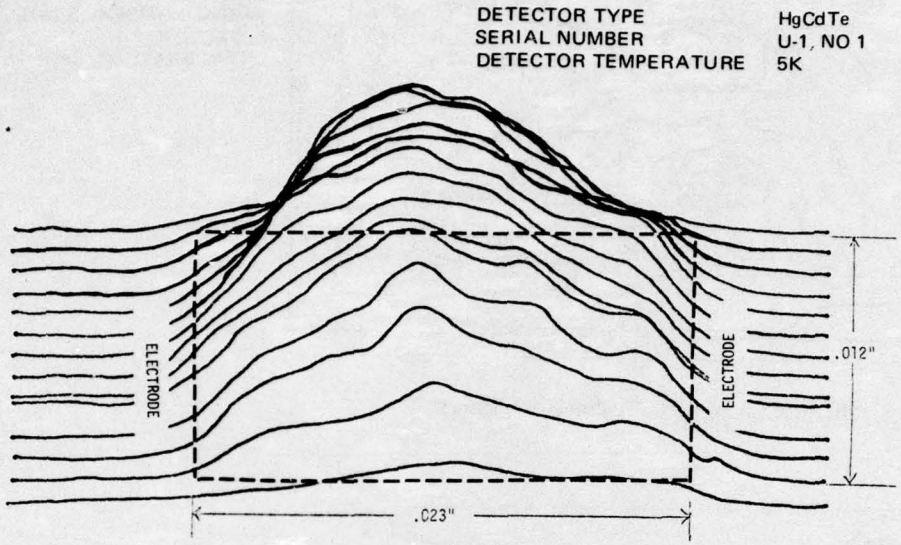

Figure 3. Element 1 of a six-element HgCdTe array.

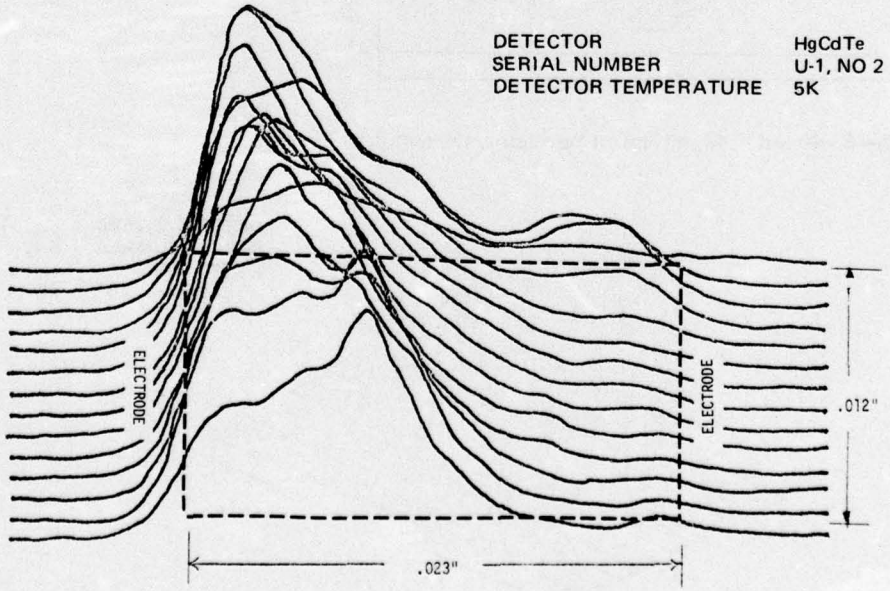

Figure 4. Element 2 of a six-element HgCdTe array.

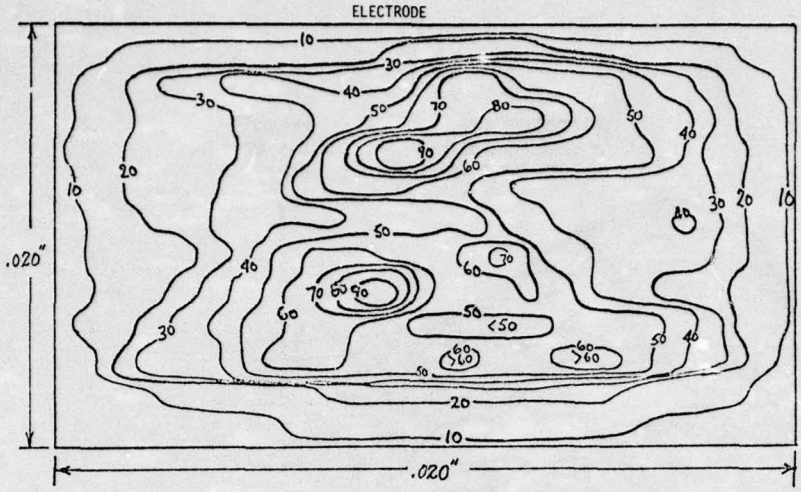

DETECTOR TYPE HgCdTe
SERIAL NUMBER 5-14-32-H2, NO 2
DETECTOR TEMPERATURE 5K

Figure 5. 20 mil × 20 mil HgCdTe detector, element 2.

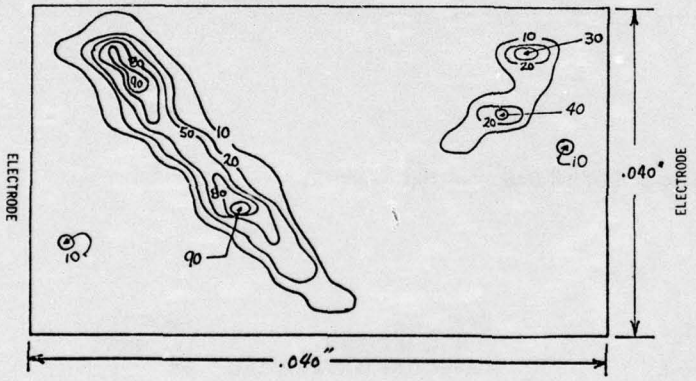

DETECTOR TYPE HgCdTe
SERIAL NUMBER S-12-49, NO 2
DETECTOR TEMPERATURE 5K

Figure 6. 40 mil × 40 mil HgCdTe detector, element 2.

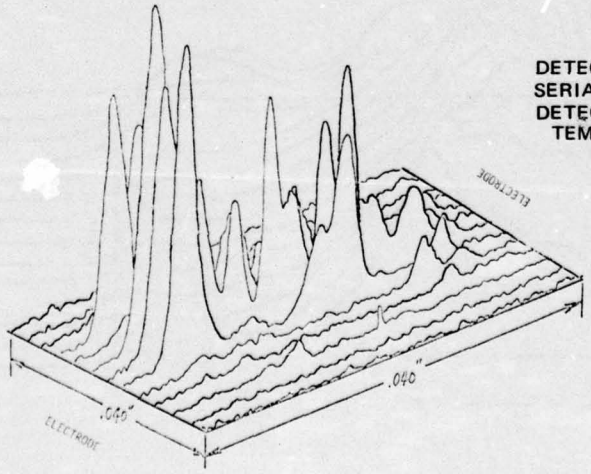

DETECTOR TYPE HgCdTe
SERIAL NUMBER S-12-49, NO 3
DETECTOR TEMPERATURE 5K

Figure 7. 40 mil × 40 mil HgCdTe detector, element 3.

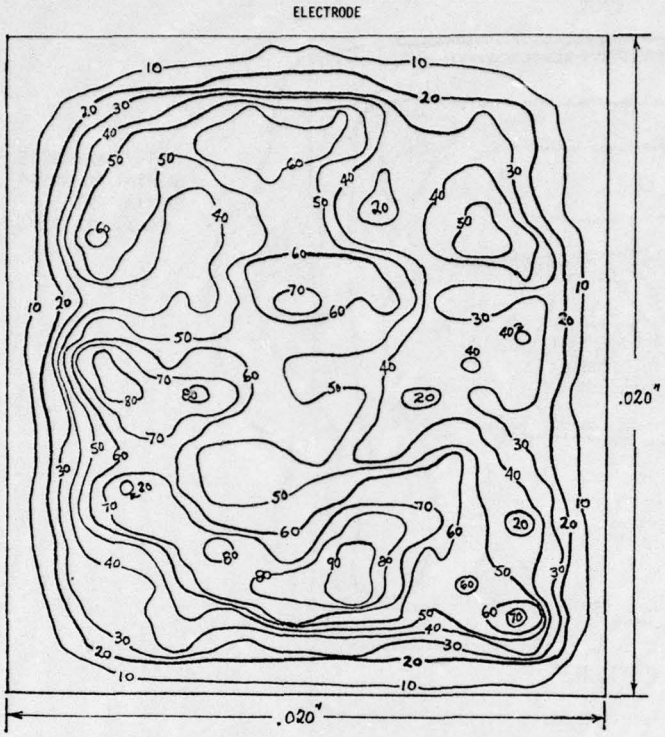

DETECTOR TYPE HgCdTe
SERIAL NUMBER S-14-39, NO 4
DETECTOR TEMPERATURE 5K

Figure 8. Element 4 of a five-element HgCdTe array.

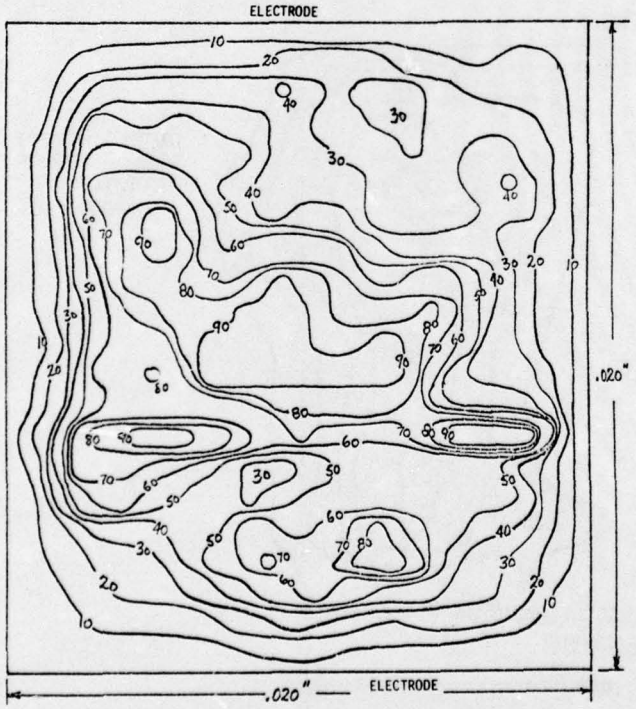

DETECTOR TYPE HgCdTe
SERIAL NUMBER S-14-39, NO 5
DETECTOR TEMPERATURE 5K

Figure 9. Element 5 of a five-element HgCdTe array.

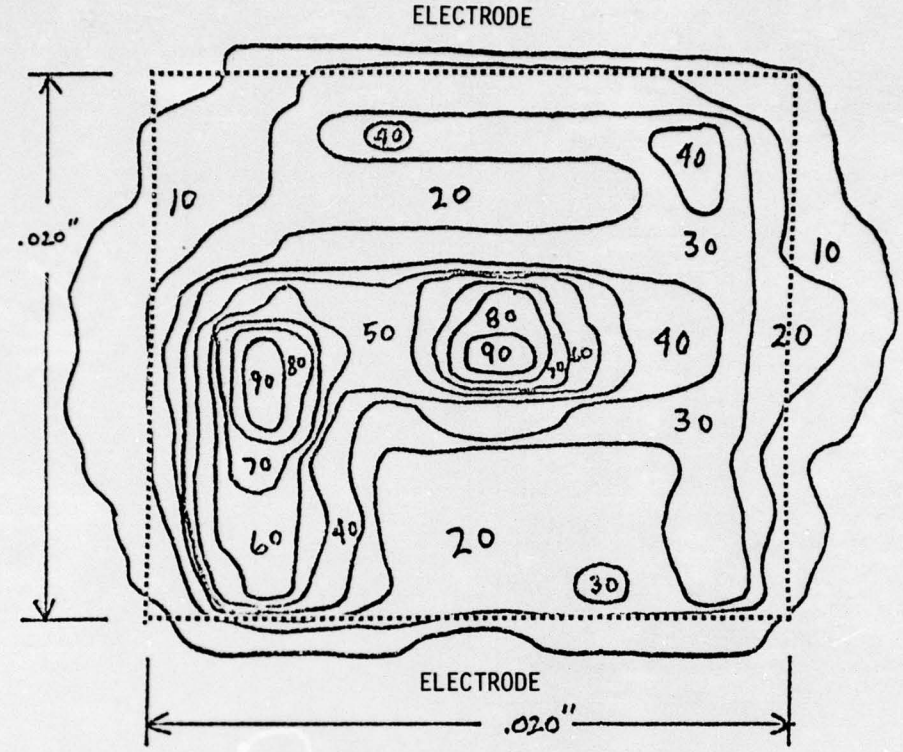

DETECTOR TYPE HgCdTe
SERIAL NUMBER S-20-38, NO 3
DETECTOR TEMPERATURE 5K

Figure 10. Element 3 of a five-element HgCdTe array.

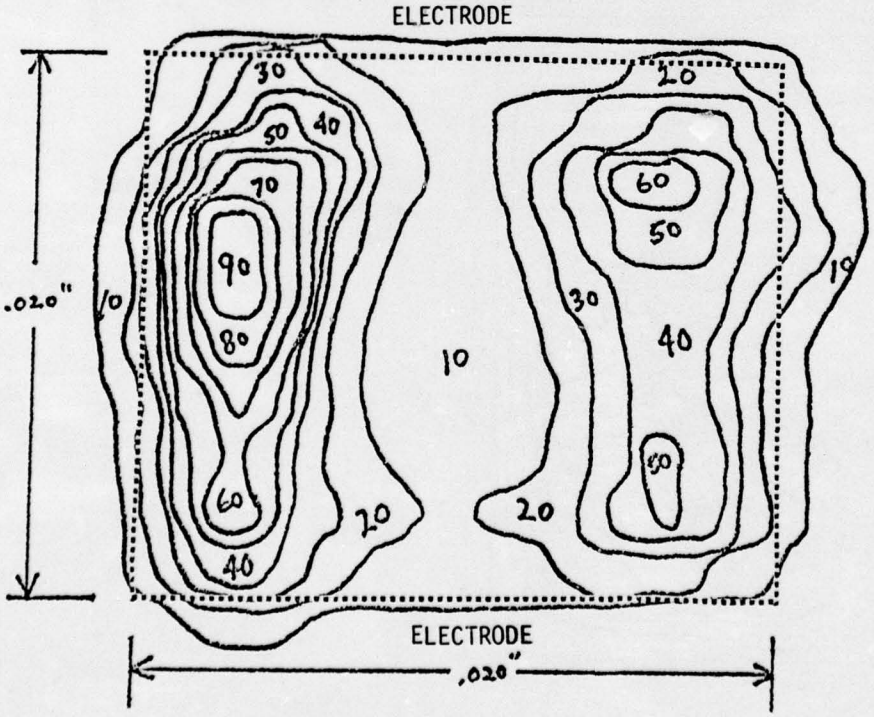

DETECTOR TYPE HgCdTe
SERIAL NUMBER S-20-38, NO 4
DETECTOR TEMPERATURE 5K

Figure 11. Element 4 of a five-element HgCdTe array.

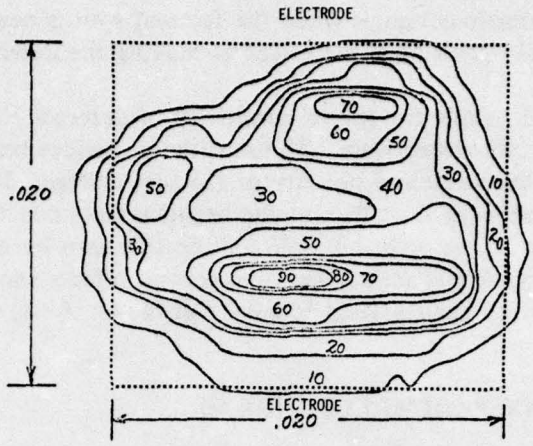

Figure 12. 20 mil X 20 mil HgCdTe detector, element 6.

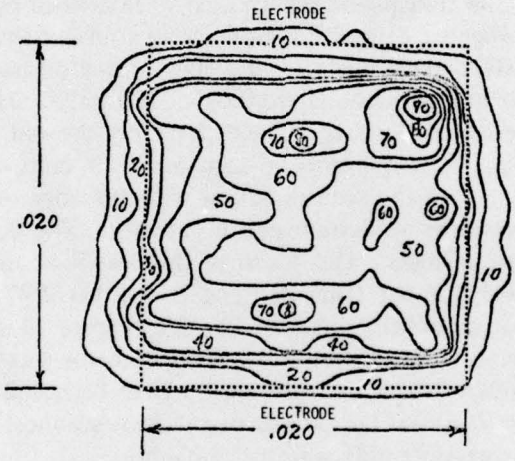

Figure 13. 20 mil X 20 mil HgCdTe detector, element 7.

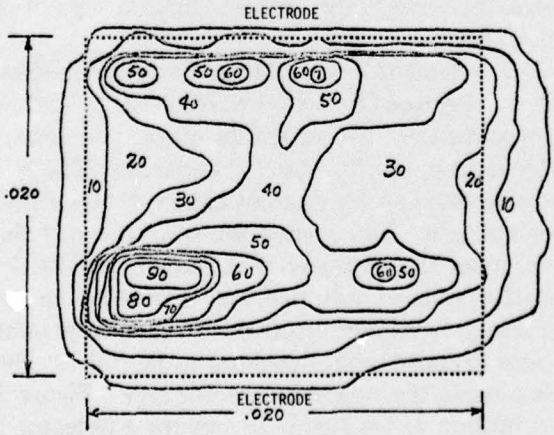

Figure 14. 20 mil X 20 mil HgCdTe detector, element 8.

the detector, give rise to anomalous signals when the focused spot is near the nominal active area. These additional signals have the effect of making the detector "look" larger than one would expect.

Figures 15, 16, and 17 show the spatial sensitivity of detector ELMS 200 at bias voltages of +5, -5, and -10 volts respectively. The sensitivity, besides being nonuniform, is seen to be dependent on the value and polarity of the bias voltage. In particular, the area of greatest sensitivity seems to shift toward the negative electrode to a degree dependent on the bias. The effect of the reflected light can also be seen by comparing the "sensitive" area with the geometrical area. The same general effects can be seen for detector HST 036, which is shown in figures 18, 19, and 20 at biases of +8, +3, and -3 volts.

EXTRINSIC SILICON–TRANSPARENT ELECTRODES

Data are shown for six detectors fabricated with transparent electrodes. All detectors of this type were made from a piece of silicon larger than the desired detector size. The active areas (under the transparent electrodes) were defined by means of an evaporated metallic pattern. Figures 21 and 22 show the spatial sensitivity of two elements of a 10-element array (HFP 042) made from a single piece of arsenic-doped silicon (monolithic). The detector dimensions are 0.012″ X 0.032″. The data show extremely good uniformity across the surface. These detectors showed good uniformity over a wide range of bias values. The nonuniform scans near the ends of the detectors were due to a slight misalignment of the scan direction with the edge of the detector.

Figure 23 shows the data for a silicon-bismuth detector. The detector is in the shape of a truncated equilateral triangle. The width of the base is about 0.019″ and the altitude is 0.270″. The width at the truncated end is about 0.003″. The measured element is one of an 8-element monolithic array (LTV-12). Figure 24 shows data on an arsenic-doped silicon detector of similar dimensions. This detector was also one element of an 8-element array (VSD B224-01). Good uniformity is to be noted for both of these detectors. Because of mechanical limitations of the spot scanner, scans over the entire sensitive areas of these two detectors were not possible.

Data on one element of a 5-element monolithic array of Si:As detectors are shown in figures 25, 26, and 27. The area of this detector was 0.020″ X 0.020″. Data are shown at three different flux levels (varying over three orders of magnitude) and good uniformity is seen in all cases.

Data for one element of a 5-element monolithic Si:Bi array are shown in figures 28, 29, and 30. The data shown in figures 28 and 29 were obtained with a bias of -10 volts and two flux levels approximately two orders of magnitude apart. The distinct nonuniformity as well as the dependence on flux level is apparent. These data can be qualitatively explained by assuming that the transparent electrode has a resistance which approaches that of the detector material. Thus, when the spot of signal flux strikes the detector it lowers the resistance under the spot and thus reduces the local electric field. Conversations with the manufacturers have confirmed that difficulties in certain manufacturing processes can lead to a high resistance electrode. Visual inspection of the opaque film surrounding the sensitive area revealed what appeared to be holes. These holes undoubtedly produced the signals outside the nominal detector area. Figure 30 shows the detector under the same flux condition as for figure 29 but for a detector bias of -5 volts.

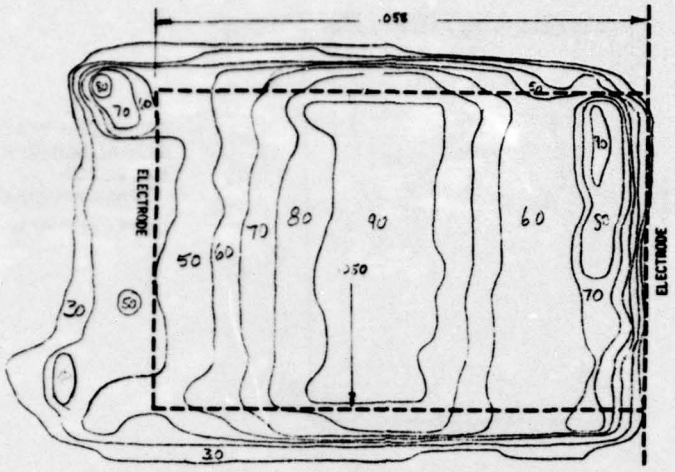

DETECTOR TYPE Si:As
SERIAL NUMBER ELMS-200
DETECTOR TEMPERATURE 5K
DETECTOR BIAS +5 V

Figure 15. 58 mil X 50 mil Si:As detector, +5 volts bias.

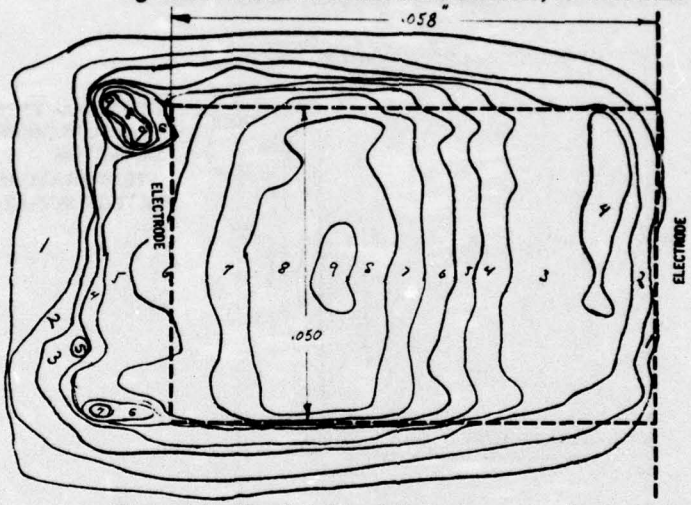

DETECTOR TYPE Si:As
SERIAL NUMBER ELMS-200
DETECTOR TEMPERATURE 5K
DETECTOR BIAS -5V

Figure 16. 58 mil X 50 mil Si:As detector, -5 volts bias.

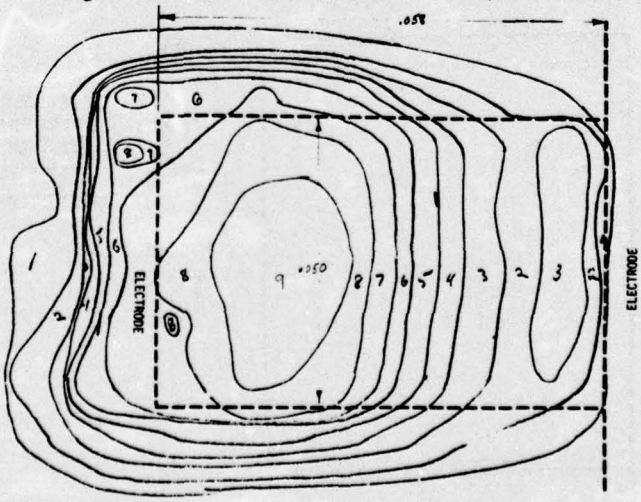

DETECTOR TYPE Si:As
SERIAL NUMBER ELMS-200
DETECTOR TEMPERATURE 5K
DETECTOR BIAS -10V

Figure 17. 58 mil X 50 mil Si:As detector, -10 volts bias.

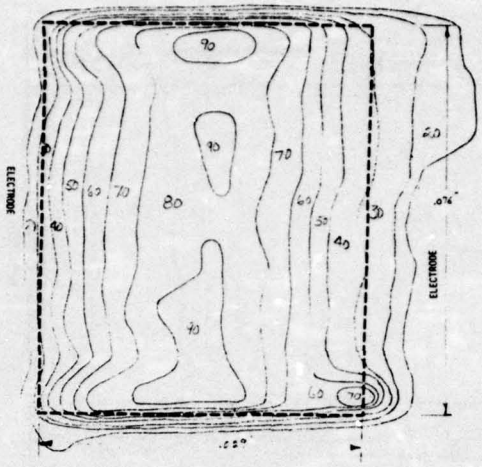

DETECTOR TYPE	Si:As
SERIAL NUMBER	HST-036
DETECTOR TEMPERATURE	5K
DETECTOR BIAS	+8V

Figure 18. 29 mil X 76 mil Si:As detector, +8 volts bias.

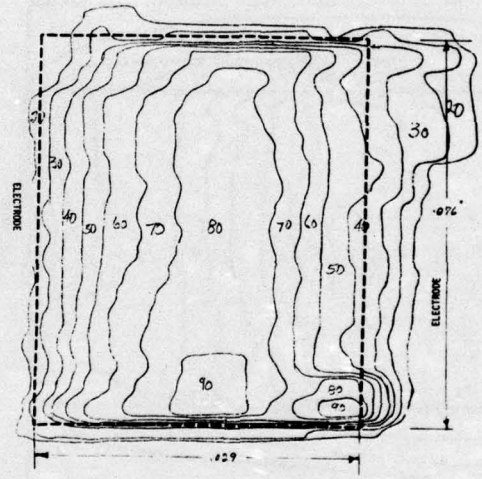

DETECTOR TYPE	SiAs
SERIAL NUMBER	HST-036
DETECTOR TEMPERATURE	5K
DETECTOR BIAS	+3V

Figure 19. 29 mil X 76 mil Si:As detector, +3 volts bias.

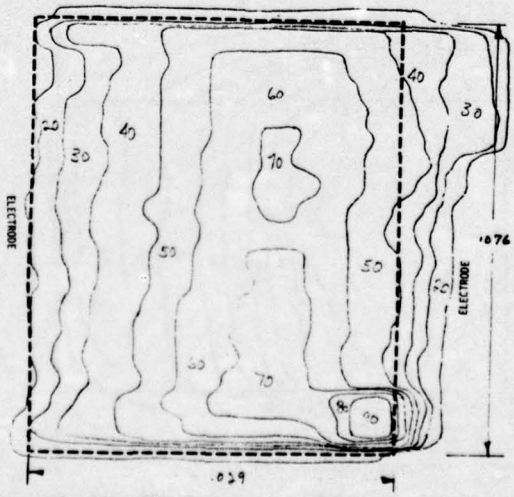

DETECTOR TYPE	Si:As
SERIAL NUMBER	HST-036
DETECTOR TEMPERATURE	5K
DETECTOR BIAS	-3V

Figure 20. 29 mil X 76 mil Si:As detector, -3 volts bias.

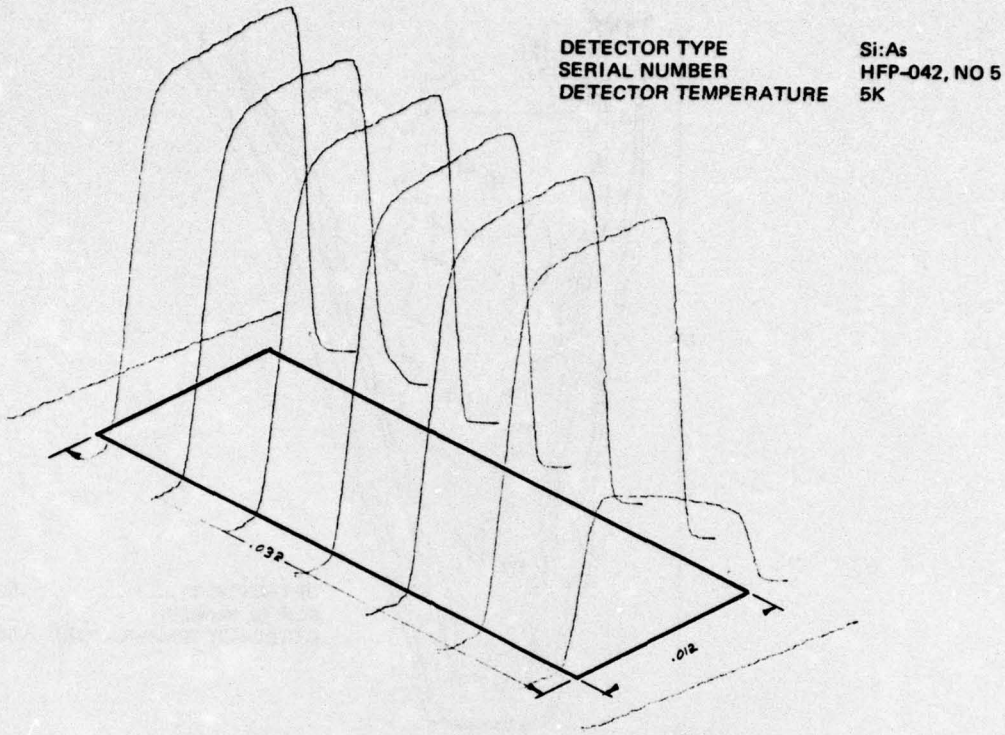

Figure 21. Element 5 of a 10-element Si:As monolithic array.

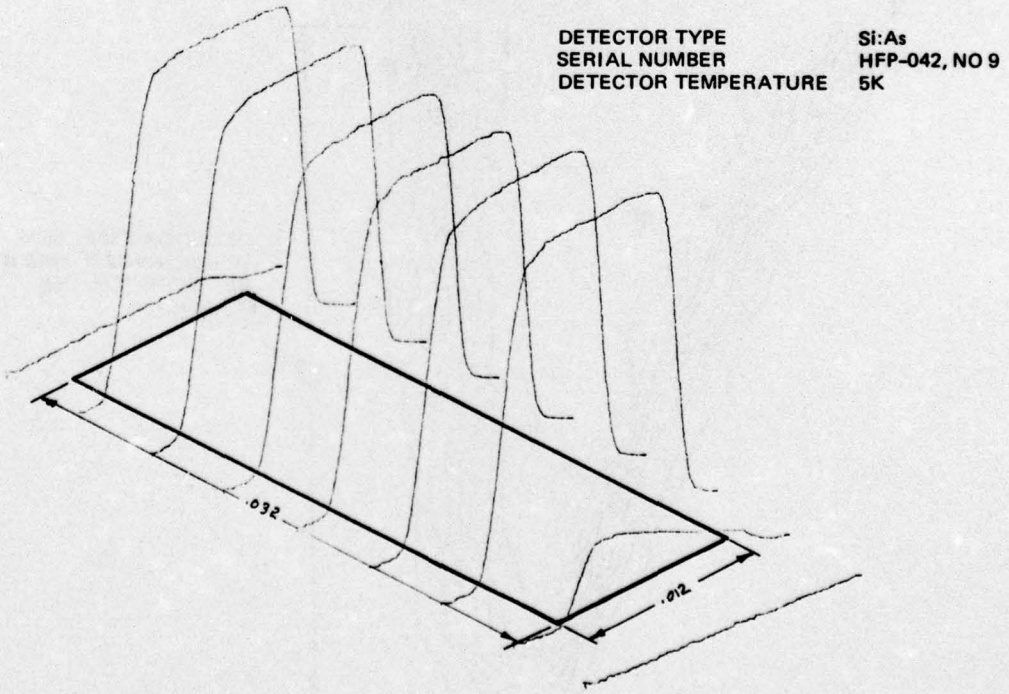

Figure 22. Element 9 of a 10-element Si:As monolithic array.

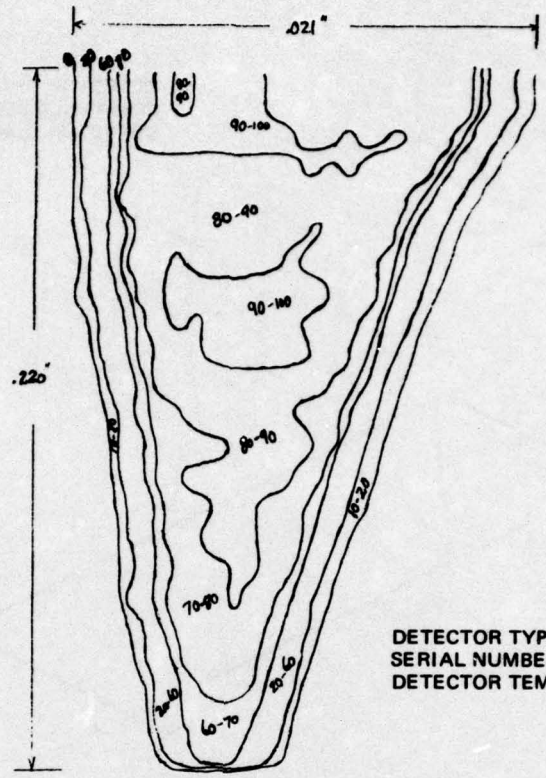

Figure 23. Si:Bi detector fabricated with transparent electrodes.

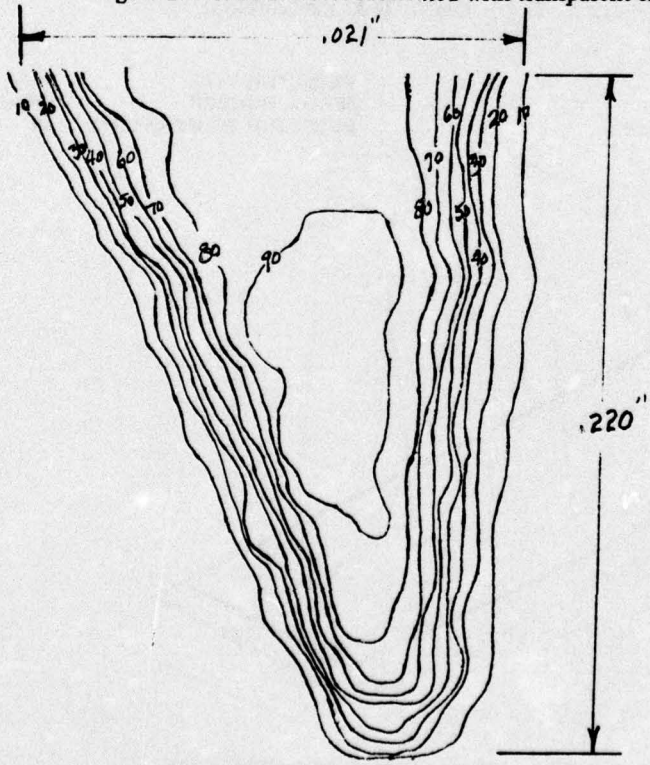

Figure 24. Si:As detector fabricated with transparent electrodes.

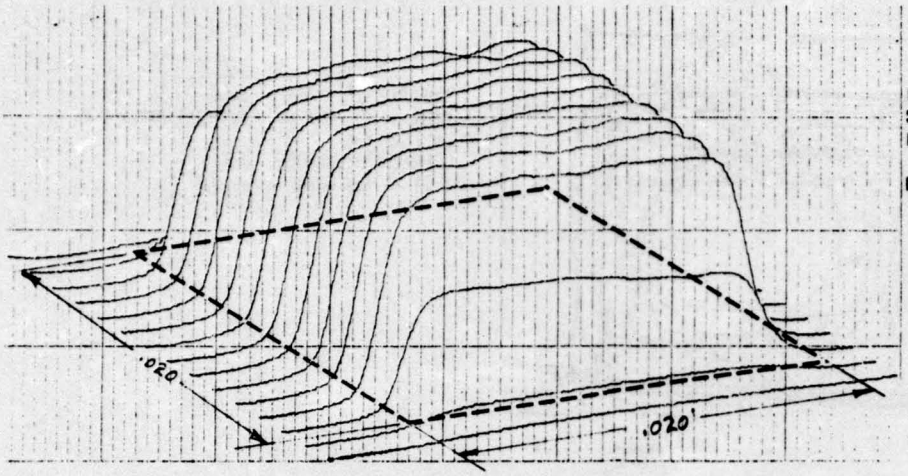

Figure 25. Si:As detector with transparent electrodes, maximum signal of 8 millivolts.

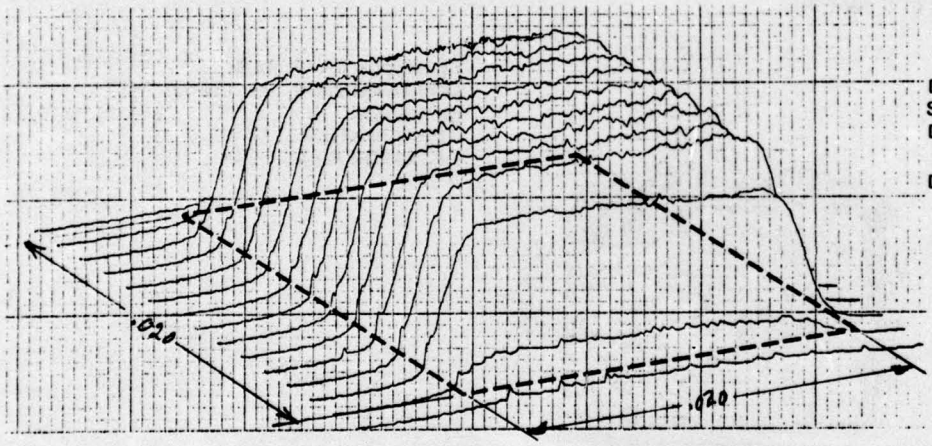

Figure 26. Si:As detector with transparent electrodes, maximum signal of 800 microvolts.

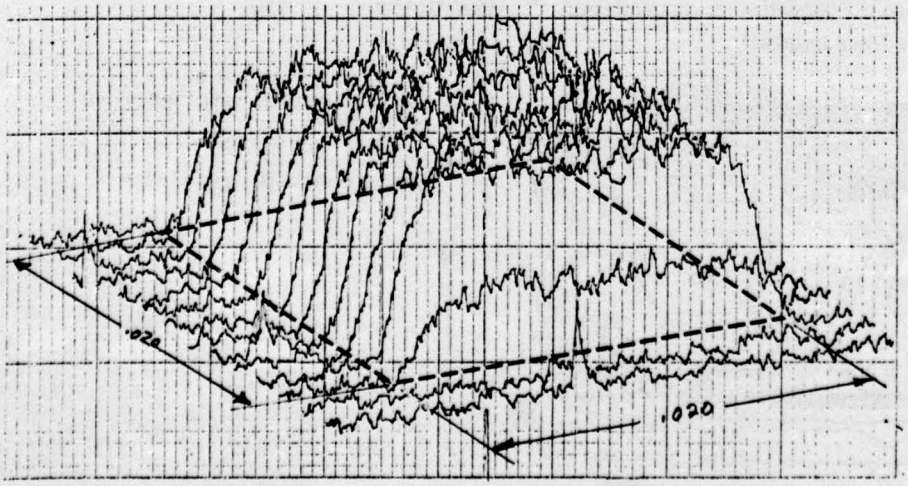

Figure 27. Si:As detector with transparent electrodes, maximum signal of 8 microvolts.

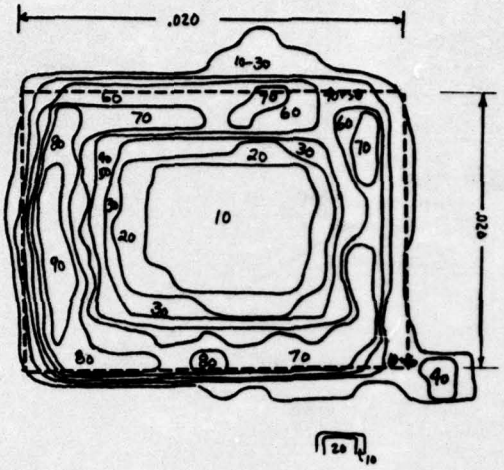

Figure 28. Si:Bi detector with defective transparent electrode, -10 volts bias and a maximum signal of 8 millivolts.

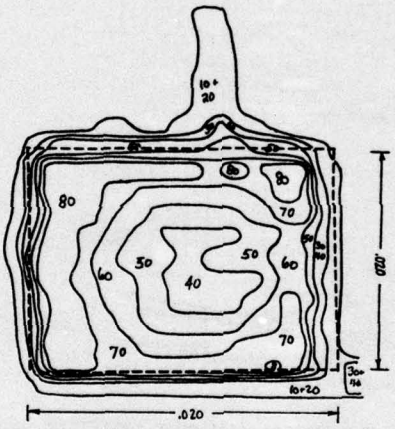

Figure 29. Si:Bi detector with defective transparent electrode, -10 volts bias and a maximum signal of 80 microvolts.

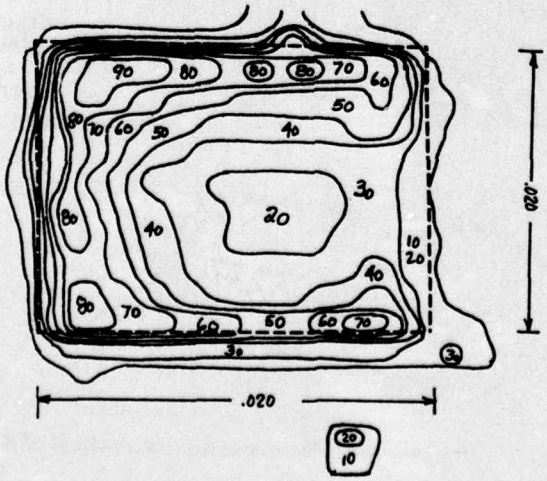

Figure 30. Si:Bi detector with defective transparent electrode, -5 volts bias and a maximum signal of 80 microvolts.

CONCLUSIONS

The spatial sensitivities of 32 low-background photoconductive HgCdTe detector elements have been measured to date. In all cases the data have shown substantial variations in signal amplitude over the sensitive area of the detector. Signal variations of 50% over a distance of a few mils are not uncommon. In several instances the spatial structure appeared to be limited by the 2-mil-diameter spot used to obtain the data. In the worst cases, less than half of the geometrical area of the detectors exhibited any appreciable photoresponse.

Several extrinsic low-background detectors have been measured. The spatial characteristics of extrinsic detectors are dependent upon the geometry of the bias field. The spatial characteristics of detectors having the bias field perpendicular to the incident radiation are dependent upon the magnitude and polarity of the applied bias. Other data[1] indicate that the spatial sensitivity of detectors of this type will be dependent upon the spectral and temporal characteristics of the signal radiation as well as upon several other operating parameters.

Few extrinsic detectors utilizing transparent electrodes have been measured. The limited data indicate that this type of detector can have good performance characteristics and uniform spatial sensitivity. However, the transparent electrode must have a relatively low resistivity in order to produce satisfactory performance.

[1] "Characteristics of Detectors Having Partially Illuminated Sensitive Areas," C Sayre, *et al*, Minutes of the Meeting of the IRIS Specialty Group on IR Detectors, 1976, Environmental Research Institute of Michigan

INITIAL DISTRIBUTION LIST

BALLISTIC MISSILE DEFENSE ADVANCED TECHNOLOGY CENTER
ATC-S, M CAPPS
ATC-O, F HOKE
ATC-O, T BOWEN

BALLISTIC MISSILE DEFENSE PROGRAM OFFICE
DACS-BMT

US ARMY COMBAT DEVELOPMENT COMMAND
TECHNICAL LIBRARY

US ARMY ELECTRONICS COMMAND
DRSEL-CT-L-C, CLAIR BURKE

ARMY MATERIALS AND MECHANICS RESEARCH CENTER
AMXMR-H, DR JA HOFMANN
AMXMR-PL (2)
AMXMR-AP
AMXMR-PR
AMXMR-CT

US ARMY MATERIEL COMMAND
AMCRD-TT, R ZENTNER

US ARMY MISSILE COMMAND
AMCPM-MDEI, A OLDSHAKER
AMSMI-RR, L LIVELY
AMSMI-RRC, G SAKELLRIDES

US ARMY FOREIGN SCIENCE & TECHNOLOGY CENTER
DAN BARNEY

US ARMY NIGHT VISION LABORATORY
TECH LIBRARY

BALLISTIC MISSILE DEFENSE SYSTEMS COMMAND
BMDSC-TEN, NOAH HURST

HARRY DIAMOND LABORATORIES
AMXDO-RC, DR R OSWALD
AMXDO-NP, DR F WIMENITZ
AMXDO-RF, E CONRAD

OFFICE OF THE CHIEF OF RESEARCH DEVELOPMENT & ACQUISITION
HQDA (DAMA-CSS-D/DR J BRYANT)

AIR FORCE MATERIALS LABORATORY
AFML/LPO, R HICKMOTT

AIR FORCE CAMBRIDGE RESEARCH LABORATORIES
LQD STOP 30, DR FD SHEPHERD, JR

AIR FORCE AVIONICS LABORATORY
AFAL/TEO
T PICKENPAUGH
DON PEACOCK
JD PARKER
LH MEUSER

AIR FORCE SPACE AND MISSILE SYSTEMS ORGANIZATION
DYS, CAPT WAYNE SCHOBER (2)
DYJ, JV KENNEDY
XRTS, JE HENGLE
DYJT, H STEARS
DYD, CR SCHEERER
SYS, RH WEBER
SZJ, COL SCHULTZ

AIR FORCE WEAPONS LABORATORY
AIR FORCE SYSTEMS COMMAND
WLRP, LTC D YOUNG

DEFENSE ADVANCED RESEARCH PROJECTS AGENCY
CAPT J JUSTICE
DR DE MANN

DEFENSE NUCLEAR AGENCY
SPAS, CAPT R DAVIS

OFFICE OF THE DIRECTOR OF DEFENSE RESEARCH AND ENGINEERING
J PERSH, DEPUTY FOR MATERIALS & STRUCTURES (ENGINEERING TECHNOLOGY)
ASST DIRECTOR
DEPUTY DIRECTOR (S&SS)
C McLAIN (SW)
DJ BROCKWAY (DS)
E MEYERS

INSTITUTE OF DEFENSE ANALYSIS
AD SCHNITZLER

CHIEF OF NAVAL OPERATION
NOP-972, F TOWERY
CAPT SEARL

NAVAL AIR SYSTEMS COMMAND
NAIR-03B
NAIR-633
NAIR-604 (2)

NAVAL AIR DEVELOPMENT CENTER
LIBRARY
CODE 202, MRS RG MANDRACK

NAVAL ELECTRONIC SYSTEMS COMMAND
NELEX 301
NELEX 51013
PME-121

NAVAL SEA SYSTEMS COMMAND
NSEA-0352, M KINNA
NSEA-0321
NSEA-034
NSEA-03522
NSEA-2052

OFFICE OF NAVAL RESEARCH
ONR-421
ONR-461

NAVAL RESEARCH LABORATORY
CODE 6460, DR BJ FARADAY
DR ND WILEY
CODE 5504.5, AF MILTON
CODE 7128
CODE 7300
CODE 5500, DR SOOY
CODE 5554, DR LEON ESTEROWITZ
DR FILBERT BARTOLI

NAVAL SURFACE WEAPONS CENTER
WHITE OAK

NAVAL SURFACE WEAPONS CENTER
DAHLGREN LABORATORY
TECH LIBRARY

NAVAL WEAPONS CENTER
TECH LIBRARY

ENVIRONMENTAL RESEARCH INSTITUTE OF MICHIGAN
IRIA LIBRARY

LOS ALAMOS SCIENTIFIC LABORATORY
GMX-6, DR JW TAYLOR

MASSACHUSETTS INSTITUTE OF TECHNOLOGY
LINCOLN LABORATORY
G COTTON
DR LONGAKER
AD GSCHWENDTNER

RIVERSIDE RESEARCH INSTITUTE
TOM LIBRARY
S CUTLER
GARY GLASER

UNIVERSITY OF ARIZONA
SECURITY OFFICER
W WOLF

UNIVERSITY OF DENVER
DENVER RESEARCH INSTITUTE
DG MURCRAY

AEROJET ELECTROSYSTEMS CO
BLDG 53, DEPT 5201, DR C PARRY
LIBRARY ACQUISITIONS

AEROSPACE CORP
EL SEGUNDO OPERATIONS
H GRAFF
RG SHEFFER

ARO, INC
F ARNOLD
ARNOLD AF STATION

THE BOEING COMPANY
AEROSPACE GROUP
MAIL STOP 8H12, DR K NORSWORTHY

BARNES ENGINEERING CO
DEFENSE & SPACE DIVISION
TECHNICAL LIBRARY

BECKMAN INSTRUMENTS, INC
RESEARCH LIBRARY

GENERAL DYNAMICS/POMONA
DIVISION LIBRARY, MZ 4-20
WR BURK

GENERAL ELECTRIC CO
OPTOELECTRONIC SYSTEMS OPERATION
PE HOWARD

GENERAL ELECTRIC CO
VALLEY FORGE SPACE TECHNOLOGY CENTER
K HALL

GENERAL ELECTRIC/TEMPO
MACK STANTON

SPARTAN RESEARCH ASSOCIATES
J GEANAKOS

HONEYWELL SYSTEMS & RESEARCH CENTER
R HEINISCH

HONEYWELL, INC
RADIATION CENTER
J SCHLICKMAN
M REINE
TTS WONG

HUGHES AIRCRAFT COMPANY
G AROYAN
R HEDDEN
KE MEYERS
JF HEINTZ
G AUTIO

HUGHES RESEARCH LABORATORY
GS PICUS

INTELCOM RAD TECH
DR JA NABER
DR A KALMA

KAMAN SCIENCES CORPORATION
PL JESSEN

LOCKHEED MISSILES AND SPACE COMPANY
K CUFF

LTV AEROSPACE CORPORATION
MISSILES AND SPACE DIVISION
WC McMILLIN
AB WELCH
CV KRAMES

ARTHUR D LITTLE, INC
DR DANIEL STANFILL, 14F/305

McDONNELL DOUGLAS ASTRONAUTICS COMPANY
HUNTSVILLE, AL
R NICHOLS

McDONNELL DOUGLAS ASTRONAUTICS COMPANY
HUNTINGTON BEACH, CA
R HARTMAN
I RICHMAN

MISSION RESEARCH CORPORATION
DR ROY HENDRICK

PHILCO-FORD CORPORATION
AERONUTRONICS DIVISION
K ATTINGER
J ROSCHEN

OPTICAL SCIENCE CONSULTANTS
DL FRIED

THE RAND CORPORATION
SANTA MONICA, CA
DR H LEIFER

ROCKWELL INTERNATIONAL CORPORATION
AUTONETICS DIVISION
ELECTRO OPTICAL LABORATORY
G HOOVER
R FLORENCE
RE HOVDA
R NELSON

SANTA BARBARA RESEARCH CENTER
D BODE

SOUTHWEST RESEARCH INSTITUTE
A WENZEL

SPECTRONICS, INC
BILLY COTTONGIN

TELEDYNE BROWN ENGINEERING COMPANY
GR EZELL

PERKIN-ELMER CORPORATION
DP MATHUR, MAIL STOP 218

TEXAS INSTRUMENTS, INC
S BORRELLO

NATIONAL BUREAU OF STANDARDS
OPTICS METROLOGY BRANCH
H KOSTKOWSKI

NASA FLIGHT RESEARCH CENTER
EDWARDS AFB

NASA GODDARD SPACE FLIGHT CENTER
GREENBELT, MD
TRACKING SYST DIV, OPTICAL SYST BRANCH
731, IT GOLDBERG
524, SH GENATT

NASA, LANGLEY RESEARCH CENTER
JA DODGEN
WD HESKETH
RK CROUCH

NASA LEWIS RESEARCH CENTER

NASA LYNDON B JOHNSON SPACE CENTER
TECH LIBRARY - BM6

MC DONNELL DOUGLAS CORP
BILL DUBOIS
ST LOUIS, MO

DEFENSE DOCUMENTATION CENTER (12)